Journal of Solid State Chemistry 183 (2010) 2222–2226

Contents lists available at ScienceDirect

Journal of Solid State Chemistry

journal homepage: www.elsevier.com/locate/jssc

Structure and photoluminescence of Mg–Al–Eu ternary hydrotalcite-like layered double hydroxides

Yufeng Chen [a,*], Fei Li [a], Songhua Zhou [a], Junchao Wei [a], Yanfeng Dai [a], Yiwang Chen [a,b,**]

[a] Department of Chemistry, Nanchang University, Nanchang 330031, China
[b] Institute of Polymers, Nanchang University, Nanchang 330031, China

ARTICLE INFO

Article history:
Received 19 May 2010
Received in revised form
14 July 2010
Accepted 25 July 2010
Available online 1 August 2010

Keywords:
Mg–Al–Eu ternary LDHs
Photoluminescence
Eu ions emissions

ABSTRACT

A series of Mg–Al–Eu ternary hydrotalcite-like layered double hydroxides (LDHs), with Eu/Al atomic ratios of ~0.06 and Mg/(Al+Eu) atomic ratios ranging from 1.3 to 4.0, were synthesized by a coprecipitation method. The Mg–Al–Eu ternary LDHs were investigated by various techniques. X-ray diffraction (XRD) results indicated that the crystallinity of the ternary LDHs was gradually improved with the increase of $Mg^{2+}/(Al^{3+}+Eu^{3+})$ molar ratio from 1.3/1 to 4/1, and all the samples were a single phase corresponding to LDH. The photoluminescent (PL) spectra of the ternary Mg–Al–Eu LDHs were described by the well-known $^5D_0$–^7F_J transition (J=1, 2, 3, 4) of Eu^{3+} ions with the strongest emission for J=2, suggesting that the host LDH was favorable to the emissions of Eu^{3+} ions. The asymmetry parameter (R) relevant to $^5D_0$–^7F_J transition (J=1, 2) dependant of the atomic ratios of $Mg^{2+}/(Al^{3+}+Eu^{3+})$ was discussed, and was consistent with the result of XRD.

1. Introduction

Layered double hydroxides (LDHs) have attracted increasing attention owing to their potential industrial applications as anion ion-exchangers, adsorbents, catalyst, and functional materials [1–5]. LDHs consist of positively charged brucite-like layers, where a fraction of the divalent cations was replaced by trivalent cations [6]. Up to now, most of the studies on MgAl-LDHs were focused on ion-exchanges [7], organic-intercalation [8,9], exfoliation/self-assembly [10,11], etc. For the application of fluorescent probe in biology or medical diagnosis, rare earth ions doped into the layers of LDHs should be meaningful.

Rare-earth doped materials, such as nanocrystals or complexes, have been extensively studied [12–14]. Among the RE ions, trivalent europium ion was a well-known dopant for many compounds, producing red emissions [12,13]. These materials possessed a variety of applications including phosphors, display monitor, X-ray imaging, scintillators, optical communication, fluorescence imaging, etc. [15–17].

Recently, some researches about the intercalation of rare earth ions complex into interlayer of LDHs have been reported [18–21], and some rare earth layered hydroxides have been synthesized [22–25]. However, to the best of our knowledge, the study on Mg–Al–Eu ternary hydrotalcite-like LDHs was hardly reported. In views of cheap raw and simple processing, we have investigated the synthesis and photoluminescence properties of Mg–Al–Eu ternary LDHs in this paper. It will be a candidate for the fluorescent probes applied in biology or medical diagnosis by varied photoluminescent properties resulted from different interlayer guests, and the probe fabricated with inorganic materials may possess better thermal stability and less toxicity than those probes fabricated with organic materials.

2. Experimental section

2.1. Sample preparation

$MgCl_2$, $AlCl_3 \cdot 6H_2O$, Eu_2O_3, $NH_3 \cdot H_2O$, and HCl were of A.R. grade, and were purchased from Chemistry Reagent Corporation of National Medicine Group. CO_2-free deionized water was used in all experiments. $MgCl_2$, $AlCl_3 \cdot 6H_2O$, and Eu_2O_3 solid were mixed and dissolved in a ~250 mL CO_2-free HCl aqueous solution at the Mg/(Al+Eu) molar ratios of 1.3/1, 2/1, 3/1, and 4/1, respectively, and an Eu/Al molar ratio of 0.06 was maintained. Then, a series of Mg–Al–Eu ternary hydrotalcite-like layered double hydroxides, with Eu/Al atomic ratios of ~0.06 and Mg/(Al+Eu) atomic ratios ranging from 1.3/1, 2/1, 3/1 to 4/1, were synthesized by the coprecipitation method.

The procedure was followed as $NH_3 \cdot H_2O$ solution was gradually dropped into the prepared mixed solutions of $MgCl_2$, $AlCl_3$, and $EuCl_3$, and continuously stirring. After precipitation

* Corresponding author. Fax: +86 791 3969513.
** Corresponding author.
E-mail addresses: yfchen@ncu.edu.cn (Y. Chen), ywchen@ncu.edu.cn (Y. Chen).

0022-4596/$ - see front matter © 2010 Elsevier Inc. All rights reserved.
doi:10.1016/j.jssc.2010.07.042

(pH ≈ 8), the slurry was filtrated, washed with CO_2-free deionize water, and dried at 90 °C for 6 h. The Mg–Al–Eu ternary products with Mg/(Al+Eu) molar ratios of 1.3/1, 2/1, 3/1, and 4/1 were signed as $Mg_{1.3}$(AlEu)-LDH, Mg_2(AlEu)-LDH, Mg_3(AlEu)-LDH, and Mg_4(AlEu)-LDH, respectively. A binary MgAl-LDH with Mg/Al molar ratio of 2/1 was prepared by the same method as above and signed as Mg_2Al-LDH.

2.2. Characterization techniques

Fourier transform infrared (FTIR) spectra of the solid materials were obtained with Shimadzu IR Prestige-21 FTIR spectrometer by the KBr method. X-ray diffraction measurements (XRD) were performed on a Bruker D8 Focus (40 kV, 40 mA) with Cu$K\alpha$ radiation; data acquisition was performed using a scan speed of 2°/min, and 2θ ranging from 4.0° to 70°.

Thermogravimetric (TG) and differential thermogravimetric (DTG) data were collected using synchronous thermal analyzer (PYRIS DIAMOVD, AMERICAN PE COMPANY) under nitrogen atmosphere at a scan rate of 10 °C/min. Chemical contents of Mg, Al, and Eu were determined by inductively coupled plasma atomic emission spectroscopy (ICP-AES, OPTIMA 5300DV, AMERICAN PE COMPANY). The chemistry formula was estimated from the results of ICP and TG analyses. The photoluminescent property of the samples was studied with the help of F-4600 FL Spectrophotometer.

3. Results and discussion

3.1. Structural characterization

The chemical compositions of the different LDHs were included in Table 1. The atomic ratios of $Mg^{2+}/(Al^{3+}+Eu^{3+})$ in the solids were almost in agreement with those in the starting materials from Table 1. The formula in the table considers that chloride was the only compensating anion and did not take into account the presence of small carbonate impurities in the interlayer space. The XRD patterns of the products were shown in Fig. 1. All the samples can be indexed to hexagonal symmetry (shown in Table 2). In light of the chemical formula and results of XRD, the interlayer space may be accommodated by two layers of water molecules. Such a bilayer hydrate interlayer structure was also found in the layered compounds with other brucite-layers, such as buserite-type manganese oxide [26], the superconducting cobalt oxide of $Na_xCoO_2 \cdot yH_2O$ [27,28], $Na_{0.3}NiO_2 \cdot 1.3H_2O$ [29,30], and hydrated chalcogenides with alkali ions $A_x(H_2O)_z[MX]_2$ [31].

The crystallinity of the Mg–Al–Eu ternary LDHs was dependant of the $Mg^{2+}/(Al^{3+}+Eu^{3+})$ molar ratios. According to the diffraction intensity of XRD, the crystallinity of the ternary LDH tended to be better while the $Mg^{2+}/(Al^{3+}+Eu^{3+})$ molar ratio varied from 1.3/1, 2/1, 3/1 to 4/1. No phase corresponding to Eu^{3+}-contained compounds was observed. This indicated that the Eu^{3+} ions may be isomorphously present in the brucite-like layer because of their favorable ionic radii (Eu^{3+} 0.95, Al^{3+} 0.51, and Mg^{2+} 0.66 Å) [32]. Meanwhile, the crystallinity of the binary Mg_2Al-LDH was higher than that of the ternary Mg_2(AlEu)-LDH due to more distortions of lattices after substitution of a part of Al^{3+} (0.51 Å) by Eu^{3+}(0.95 Å) in the LDH framework. Nijs et al. have successfully synthesized pillared [Fe(CN)$_6$]-MgAl-LDHs with different Mg^{2+}/Al^{3+} ratios (between 1.5 and 4.5) by the coprecipitation [33].

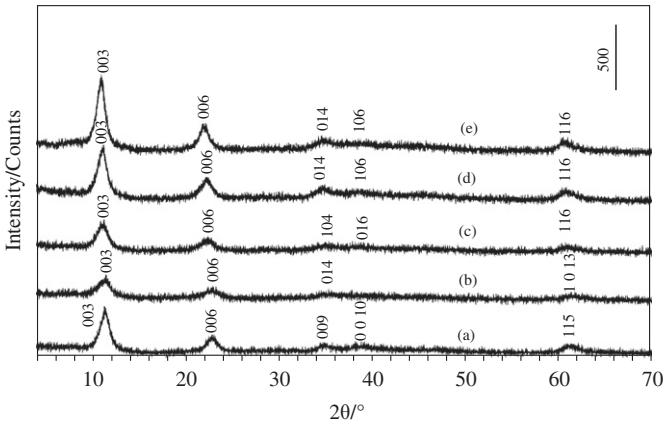

Fig. 1. XRD patterns of (a) Mg_2Al-LDH, (b) $Mg_{1.3}$(AlEu)-LDH, (c) Mg_2(AlEu)-LDH, (d) Mg_3(AlEu)-LDH, and (e)Mg_4(AlEu)-LDH.

Table 2
Lattice parameters and symmetry of LDHs.

Samples	Symmetry	Lattice parameters
Mg_2Al-LDH	Hexagonal	a=3.205(0.001), c=23.397(0.004)
$Mg_{1.3}$(AlEu)-LDH	Hexagonal	a=3.204(0.004), c=23.43(0.01)
Mg_2(AlEu)-LDH	Hexagonal	a=3.296(0.002), c=24.00(0.03)
Mg_3(AlEu)-LDH	Hexagonal	a=3.302(0.009), c=24.1(0.2)
Mg_4(AlEu)-LDH	Hexagonal	a=3.303(0.002), c=24.32(0.01)

Table 1
Compositions of the binary MgAl-LDH and ternary Mg–Al–Eu LDHs.

Samples	[a]Content (%) for found (cald.)			[b]Weight loss (%)
	Mg	Al	Eu	
Mg_2Al-LDH	20.31 (20.32)	11.44 (11.43)		10.0
Chemical formula	$Mg_2Al(OH)_6Cl \cdot 1.32H_2O$			
$Mg_{1.3}$(AlEu)-LDH	15.49(15.48)	12.56(12.59)	4.50(4.53)	10.9
Chemical formula	$Mg_{1.3}Al_{0.94}Eu_{0.06}(OH)_{4.6}Cl \cdot 1.23H_2O$			
Mg_2(AlEu)-LDH	19.65(19.63)	10.35(10.38)	3.75(3.73)	10.0
Chemical formula	$Mg_2Al_{0.94}Eu_{0.06}(OH)_6Cl \cdot 1.36H_2O$			
Mg_3(AlEu)-LDH	23.82(23.84)	8.38(8.41)	3.04(3.02)	8.0
Chemical formula	$Mg_3Al_{0.94}Eu_{0.06}(OH)_8Cl \cdot 1.33H_2O$			
Mg_4(AlEu)-LDH	26.68(26.71)	7.02(7.06)	2.49(2.54)	6.5
Chemical formula	$Mg_4Al_{0.94}Eu_{0.06}(OH)_{10}Cl \cdot 1.30H_2O$			

[a] Analyzed by ICP.
[b] Obtained from the TG curves, 20–800 °C.

The crystallographic parameters *a* and *c* of the Mg–Al–Eu ternary LDHs and Mg–Al binary LDH were calculated using the least squares method assuming a hexagonal crystal system (shown in Table 2). It can be seen that there was a small increase of *a* value with the increase of Mg content for the Mg–Al–Eu ternary LDHs. Meanwhile, the parameter *c*, which depended upon several factors such as the amount of interlayer water, crystallinity of the compound and the interaction between the layer and the interlayer, tended to be larger with the increase of Mg content. Since the synthetic parameters were constant for all the compounds, while varying only the composition of the metal ions, the increase in the *c* parameter was due to the increase of Mg content. Based on the electrostatic interactions between the layers and the anions, the larger interlayer distance was found for the sample with the higher $Mg^{2+}/(Al^{3+}+Eu^{3+})$ ratio which possessed of lower charge density. So the *c* parameter of LDHs gradually increased with the increase of $Mg^{2+}/(Al^{3+}+Eu^{3+})$ ration. In addition, the parameters *a* and *c* of the ternary Mg_2(AlEu)-LDH were slightly larger than that of the binary Mg_2Al-LDH, which was possibly owing to small parts of Al^{3+} (0.51 Å) isomorphously substituted by Eu^{3+}(0.95 Å) in the LDH framework.

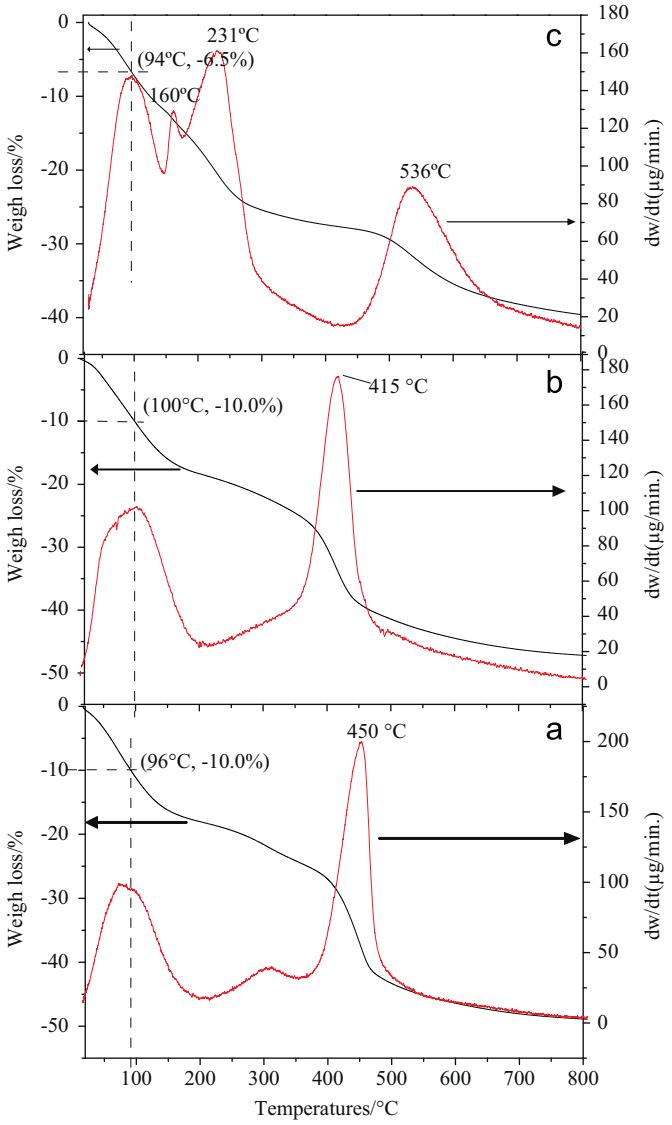

Fig. 2. TG–DTG curves of (a) Mg_2Al-LDH, (b) Mg_2(AlEu)-LDH, and (c) Mg_4(AlEu)-LDH.

3.2. Thermogravimetry and differential thermogravimetry (TG–DTG)

The TG–DTG curves of representative samples were shown in Fig. 2. There were similar weight losses in two steps for Mg_2Al-LDH and Mg_2(AlEu)-LDH, which were the characteristics of the layered double hydroxides [34]. The first loss step happened at 96–100 °C with mass losses of 10.0%, was attributed to the evaporation of physically adsorbed and interlayer water. The second loss step took place around at 410–450 °C, due to the dehydroxylation and decomposition of the interlayer small carbonate anions impurities. This behavior was accordant with that reported for MgAl-LDH(CO_3 or Cl) [34,35]. However, four mass losses were observed for the Mg_4(AlEu)-LDH. The first loss step happened at 94 °C with mass loss of 6.50%, was corresponding to the loss of the adsorbed water and the interlayer water. The second loss step and the third loss step, took place at 160 and 231 °C, respectively,

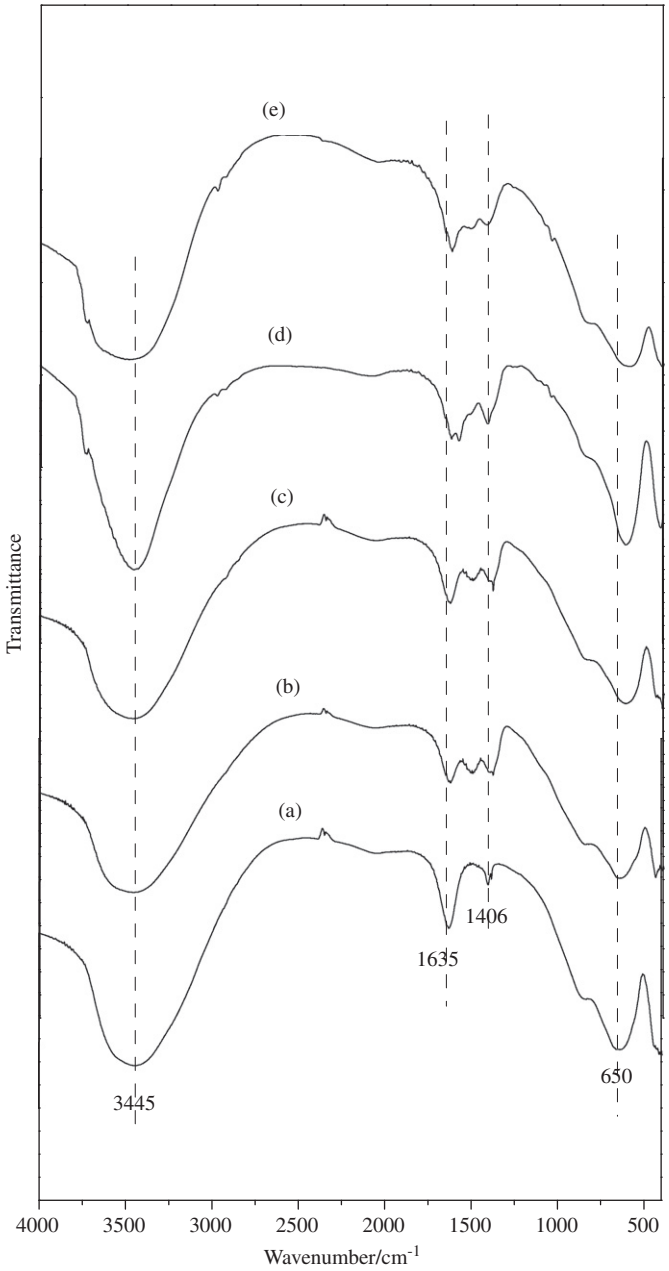

Fig. 3. IR spectra of (a) Mg_2Al-LDH, (b) $Mg_{1.3}$(AlEu)-LDH, (c) Mg_2(AlEu)-LDH, (d) Mg_3(AlEu)-LDH, and (e) Mg_4(AlEu)-LDH.

were attributed to the dehydroxylation and decomposition of the interlayer small carbonate anions impurities. The fourth stage at 536 °C was most probably due to the elimination of Cl^- intercalated in the Mg–Al–Eu LDH interlayers, similar to the decomposition of MgAl-NO_3 [36].

3.3. IR spectra

The FT-IR spectra of the LDHs samples were shown in Fig.3. An intense and broad peak at 3445 cm^{-1} was ascribed to the stretching vibration of hydroxyl groups of LDH layers and interlayer water molecules [37]. The vibration of water molecules was responsible for the band at 1635 cm^{-1}. Despite the use of CO_2-free deionized water in all experiments, a weak band in the region of 1500–1400 cm^{-1} attributed to carbonate anions [38] was observed, demonstrating that small carbon dioxides were adsorbed during the synthesis. The band close to 650 cm^{-1} was due to both Al–OH and Zn–OH translational modes [39]. These results were in agreement with that of the XRD.

3.4. Photoluminescent property

Fig.4 showed the photoluminescent spectra of the products under excitation at 380 nm. In the 530–730 nm spectral range, no emission occurred for the binary Mg_2Al-LDH, while all the Mg–Al–Eu ternary LDHs revealed the red-emitting characteristic of Eu^{3+} ions from the transitions $^5D_0$–^7F_J (J=1–4) centered around at 594, 618, 654, and 702 nm, respectively. It is well known that Eu^{3+} ions can be also used as a sensitive structural probe to detect the lattice symmetry of host materials [40]. The relative intensity of the electric-dipole $^5D_0$–$^7F_2$ transition depended on the local symmetry of Eu^{3+} ions. The intensity of this transition increased with decreasing local symmetry of the Eu^{3+} ion. The asymmetry parameter R (Eq. (1)) defined by the ratio of the area under

$$R = \frac{I\left(^5\mathrm{D}_0 - ^7\mathrm{F}_2\right)}{I\left(^5\mathrm{D}_0 - ^7\mathrm{F}_1\right)} \quad (1)$$

electric-dipole transition ($^5D_0$–$^7F_2$) to that of magnetic-dipole transition ($^5D_0$–$^7F_1$), gave information about surrounding and environmental changes around the Eu^{3+} ions. The asymmetry

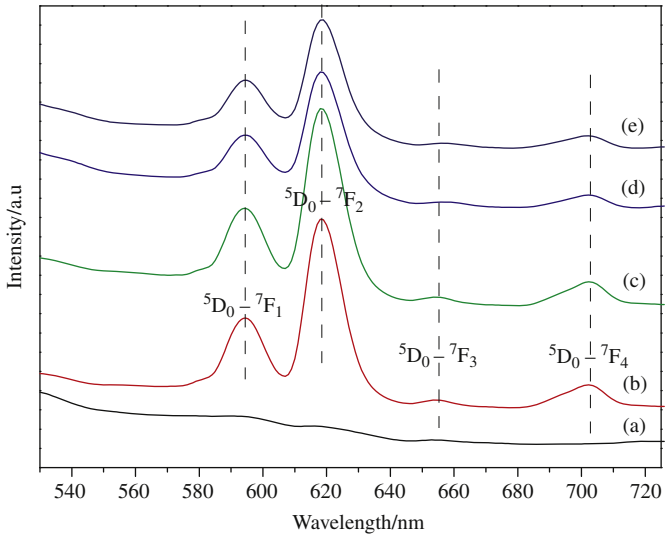

Fig. 4. Photoluminescent spectra of (a) Mg_2Al-LDH, (b) $Mg_{1.3}$(AlEu)-LDH, (c) Mg_2(AlEu)-LDH, (d) Mg_3(AlEu)-LDH, and (e) Mg_4(AlEu)-LDH.

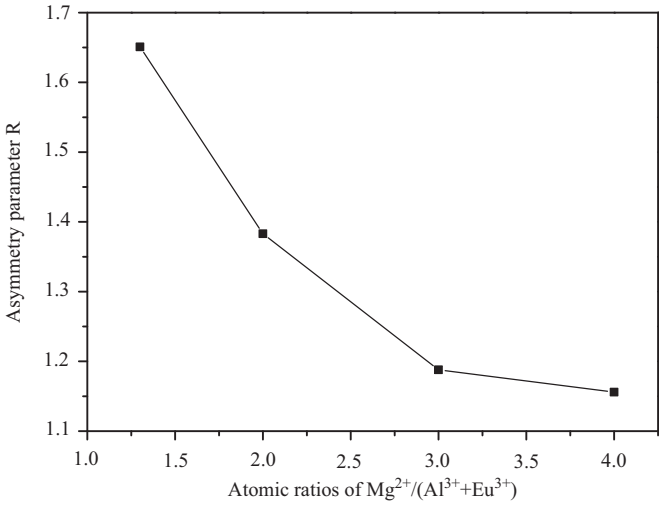

Fig. 5. Asymmetry parameter R as function of atomic ratios of $Mg^{2+}/(Al^{3+}+Eu^{3+})$.

parameter R dependant of the atomic ratios of $Mg^{2+}/(Al^{3+}+Eu^{3+})$ was presented in Fig. 5. The highest value for the sample with $Mg^{2+}/(Al^{3+}+Eu^{3+})$ atomic ratio of 1.3, suggested distorted local environment for the Eu^{3+} ion. The lowest value of the asymmetry ratio for sample with $Mg^{2+}/(Al^{3+}+Eu^{3+})$ atomic ratio of 4.0, corresponded to less distorted local environment for the Eu^{3+} ion. The asymmetry parameter R gradually decreased when the atomic ratio of $Mg^{2+}/(Al^{3+}+Eu^{3+})$ varied from 1.3, 2.0, 3.0 to 4.0, indicating the less lattice distortion in the local environment of the Eu^{3+} ion, due to less divalent metal ions (Mg^{2+}) isomorphously substituted by trivalent metal ions ($Al^{3+}+Eu^{3+}$) in the LDH framework. This result was in agreement with that of the crystallinity of samples. In all samples the $^5D_0$–$^7F_2$ transition band was dominant. The strong emission due to $^5D_0$–$^7F_2$ transition appeared when Eu^{3+} ions occupied a site without inversion symmetry. This fact suggested that Eu^{3+} ions replaced Mg^{2+} in the host lattice. The transitions $^5D_0$–^7F_J (J=1–4) was often observed in other Eu-doped systems [41,42].

4. Conclusions

In conclusion, Mg–Al–Eu ternary LDHs with various $Mg^{2+}/(Al^{3+}+Eu^{3+})$ atomic ratios of 1.3–4.0 were synthesized by the coprecipitation method. The crystallinity of the hydrotalcite materials was improved with the increase of the Mg/(Al+Eu) atomic ratio. Some intense emissions attributed to transitions $^5D_0$–^7F_J (J=1–4) of Eu^{3+} ions were observed in all ternary LDHs. The asymmetry parameter R decreased with the atomic ratio of $Mg^{2+}/(Al^{3+}+Eu^{3+})$ increasing from 1.3/1 to 4/1, suggesting the less lattice distortions in the local environment of the Eu^{3+} ion attributed to less M^{2+} (Mg^{2+}) ions isomorphously substituted by M^{3+} ($Al^{3+}+Eu^{3+}$) in the LDH framework. These results indicated that the Mg–Al–Eu LDHs may be a potential candidate for fluorescent probe applied in biological or medical diagnosis.

Acknowledgments

The Project was supported by the Natural Science Foundation of Jiangxi Province (2009GZC0085 and 2008GQH0046), National Natural Science Foundation of China (50902067), and Program for Innovative Research Team in University of Jiangxi Province.

References

[1] C. Nyambo, D. Chen, S.P. Su, C.A. Wilkie, Polym. Degradation Stability 94 (2009) 496–505.
[2] H.W. Olfs, L.O. Torres-Dorante, R. Eckelt, H. Kosslick, Appl. Clay Sci. 43 (2009) 459–464.
[3] G.L. Huang, S.L. Ma, X.H Zhao, X.J Yang, K Ooi, Chem. Mater. 22 (2010) 1870–1877.
[4] S. Velu, N. Shah, T.M. Jyothi, S. Sivasanker, Microporous Mesoporous Mater. 33 (1999) 61–75.
[5] J.F. Naime Filho, F. Silvério, M.J. dos Reis, J.B. Valim, J. Mater. Sci. 43 (2008) 6986–6991.
[6] G.G.C. Arizaga, K.G. Satyanarayana, F. Wypych, Solid State Ionics 178 (2007) 1143–1162.
[7] N. Iyi, T. Sasaki, Appl. Clay Sci. 42 (2008) 246–251.
[8] D. Carriazo, C. Domingo, C. Martin, V. Rives, Inorg. Chem. 45 (2006) 1243–1251.
[9] C. Nyambo, D. Chen, S.P. Su, C.A. Wilkie, Polym. Degradation Stability 94 (2009) 496–505.
[10] J.H. Lee, H.J. Nam, S.W. Rhee, D.-Y. Jung, Eur. J. Inorg. Chem. 36 (2008) 5573–5578.
[11] M. Szekeres, A Szechenyi, K. Stepan, T. Haraszti, I. Dekany, Colloid Polym. Sci. 283 (2005) 937–945.
[12] D.K. Williams, H. Yuan, B.M. Tissue, J. Lumin. 83 (1999) 297–300.
[13] S. Fujihara, A. Suzuki, T. Kimura, J. Appl. Phys. 94 (2003) 2411–2416.
[14] Z. Chang, D.G. Evans, X Duan, P. Boutinaud, M de Roy, C. Forano, J. Phys. Chem. Sol. 67 (2006) 1054–1057.
[15] H.X. Zhang, C.H. Kam, Y. Zhou, X.Q. Han, S. Buddhudu, Q. Xiang, Y.L Lam, Y.C. Chan, Appl. Phys. Lett. 77 (2000) 609–611.
[16] A. Patra, C.S. Friend, R. Kapoor, P.N. Prasad, J. Phys. Chem. B 106 (2002) 1909–1912.
[17] A. Mehta, T. Thundat, M.D. Barnes, V. Chhabra, R. Bhargava, A.P. Bartko, R.M. Dickson, Appl. Opt. 42 (2003) 2132–2139.
[18] F.L. Sousa, M. Pillinger, R.A. SáFerreira, C.M. Granadeiro, A.M.V. Cavaleiro, J. Rocha, L.D. Carlos, T. Trindade, H.I.S. Nogueira, Eur. J. Inorg. Chem. 4 (2006) 726–734.
[19] Z. Chang, D. Evans, X. Duan, P. Boutinaud, M. de Roy, C. Forano, J. Phys. Chem. Solids 67 (2006) 1054–1057.
[20] C. Li, L.Y. Wang, D.G. Evans, X. Duan, Ind. Eng. Chem. Res. 48 (2009) 2162–2171.
[21] L. Sarakha, C. Forano, P. Boutinaud, Opt. Mater. 31 (2009) 562–566.
[22] S.A. Hindocha, L.J. McIntyre, A.M. Fogg, J. Solid State Chem. 182 (2009) 1070–1074.
[23] L. Poudret, T.J. Prior, L.J. McIntyre, A.M. Fogg, Chem. Mater. 20 (2008) 7447–7453.
[24] F.X. Geng, Y Matsushita, R.Z. Ma, H. Xin, M. Tanaka, F. Izumi, N. Iyi, T. Sasaki, J. Am. Chem. Soc. 130 (2008) 6344–16350.
[25] L.F. Hu, R.Z. Ma, T.C. Ozawa, T. Sasaki, Inorg. Chem. 49 (2010) 2960–2968.
[26] J. Luo, Q. Zhang, A. Huang, O. Giraldo, S.L. Suib, Inorg. Chem. 38 (1999) 6106–6113.
[27] K. Takada, M. Osada, F. Izumi, H. Sakurai, E. Takayama-Muromachi, T. Sasaki, Chem. Mater. 17 (2005) 2034–2040.
[28] S. Park, Y. Lee, M. Elcombe, T. Vogt, Inorg. Chem. 45 (2006) 3490–3497.
[29] S. Park, K. Kang, W.-S. Yoon, A.R. Moodenbaugh, L.H. Lewis, T. Vogt, Solid State Commun. 139 (2006) 60–63.
[30] M.L. Foo, T. Klimczuk, L. Li, N.P. Ong, R.J. CaVa, Solid State Commun. 133 (2005) 407–410.
[31] V.R. Schöllhorn, Angew. Chem. 92 (1980) 1015–1020.
[32] R.J. Wiglusz, T Grzy, S. Lis, W. Strek, J. Lumin. 130 (2010) 434–441.
[33] H. Nijs, M. De Bock, E.F. Vansant, Microporous Mesoporous Mater. 30 (1999) 243–253.
[34] F. Cavani, F. Trifiro, A. Vaccari, Catal. Today 11 (1991) 173–301.
[35] R. Chitrakar, S. Tezuka, A. Sonoda, K Sakane, K. Ooi, T. Hirotsu, J. Colloid Interface Sci. 313 (2007) 53–63.
[36] T. Kameda, Y. Fubasami, N. Uchiyama, T. Yoshioka, Thermochim. Acta 499 (2010) 106–110.
[37] J. Wang, Q. Liu, G.C. Zhang, Z.S. Li, P.P. Yang, X.Y. Jing, M.L. Zhang, T.F. Liu, Z.H. Jiang, Solid State Sci. 11 (2009) 1597–1601.
[38] M. Badreddine, M. Khaldi, A. Legrouri, A. Barroug, M. Chaouch, A. De Roy, J.P. Besse, Mater. Chem. Phys. 52 (1998) 235–239.
[39] R.R. Delgado, C.P.D. Pauli, C.B. Carrasco, M.J. Avena, Appl. Clay Sci. 40 (2008) 27–37.
[40] J. Hölsa, E. Antic-Fidancev, M. Lastusaari, A. Lupeic, J. Solid State Chem. 171 (2003) 282–286.
[41] M.A.F. Monteiro, H.F. Brito, M.C.F. Felinto, C.M. Brito, E.E.S. Teotonio, F.M. Vichi, R. Stefani, Microporous Mesoporous Mater. 108 (2008) 237–246.
[42] Q.S. Shi, S. Zhang, Q. Wang, H.W. Ma, G.Q. Yang, W.H. Sun, J. Mol. Struct. 837 (2007) 185–189.